NIR spectrophotometric system based on a conventional CCD camera

Meritxell Vilaseca, Jaume Pujol, Montserrat Arjona
Center for Sensors, Instrumentation and Systems Development (CD6),
Dept. of Optics and Optometry, Univ. Politècnica de Catalunya,
Rambla Sant Nebridi 10, 08222 Terrassa, Barcelona, Spain

ABSTRACT

The near infrared spectral region (NIR) is useful in many applications. These include agriculture, the food and chemical industry, and textile and medical applications. In this region, spectral reflectance measurements are currently made with conventional spectrophotometers. These instruments are expensive since they use a diffraction grating to obtain monochromatic light. In this work, we present a multispectral imaging based technique for obtaining the reflectance spectra of samples in the NIR region (800 – 1000 nm), using a small number of measurements taken through different channels of a conventional CCD camera. We used methods based on the Wiener estimation, non-linear methods and principal component analysis (PCA) to reconstruct the spectral reflectance. We also analyzed, by numerical simulation, the number and shape of the filters that need to be used in order to obtain good spectral reconstructions. We obtained the reflectance spectra of a set of 30 spectral curves using a minimum of 2 and a maximum of 6 filters under the influence of two different halogen lamps with color temperatures Tc_1 = 2852K and Tc_2 = 3371K. The results obtained show that using between three and five filters with a large spectral bandwidth (FWHM ≈ 60 nm), the reconstructed spectral reflectance of the samples was very similar to that of the original spectrum. The small amount of errors in the spectral reconstruction shows the potential of this method for reconstructing spectral reflectances in the NIR range.

Keywords: CCD cameras, near infrared, infrared imaging, multispectral imaging, spectrophotometric instrumentation, industrial inspection

1. INTRODUCTION

The use of solid-state detector arrays[1] has increased rapidly in the last few years, specifically in the case of video cameras, due to their versatility and low cost. The detector can be based on various technologies, such as CCD or CMOS. The spectral response of conventional CCD cameras extends from the visible to the near infrared (NIR) and it is clearly significant up to 1000 nm. Basically, this kind of device is used for the detection of visible light, since it has the greatest sensitivity in this region, but CCD cameras with improved response in the NIR are currently manufactured. Therefore, we can make use of this standard instrumentation in NIR applications. While the visible spectrum contains very little information on the chemical composition of an object, the spectral information included in the NIR region is in general directly related to the constituents of a material. Therefore, it is used as an analytical tool in industry and research, known as NIR technology[2]. NIR technology is used in a vast number of applications. These include agriculture, the food industry, medical applications, military applications, the chemical and petrochemical industries, pharmaceutical production and laser technology[3].

Spectral reflectance measurements in the NIR region are normally made with conventional spectrophotometers. These instruments are expensive since they use a diffraction grating to obtain monochromatic light. We therefore propose an alternative methodology of spectral reflectance reconstruction using conventional CCD camera measurements. We use a method based on multispectral imaging which employs three or more acquisition channels. The use of different spectral bands, which are obtained by placing a set of filters in front of the camera, means the obtained images will have certain spectral information. With the proper mathematical treatment of these images, it is possible to reconstruct the spectral reflectance of the analyzed sample. There are various mathematical methods for reconstructing spectral data, some of them based on interpolation calculations (linear, cubic, spline, discrete Fourier transform and modified discrete sine transform approximations) and others on estimation or fitting techniques (Moore-Penrose pseudoinverse, smoothing inverse, Wiener estimation, non-linear methods and principal component analysis or characteristic vector analysis). In this study we compare the performance of these methods in the NIR region, and focus on the Wiener estimation[4-6], the

non-linear methods[7,8] and principal component analysis (PCA)[4,9-12] to reconstruct the spectral reflectance of the analyzed samples, since they generally provide better results than the other methods.

As we have mentioned, it is necessary to place a set of filters in front of the CCD camera in order to recover spectral reflectances using multispectral images. Interpolation methods require monochromatic filters in order to obtain reflectance values at different wavelengths of the spectrum. Estimation methods may use filters with different spectral features, and by extension, different transmittance values and spectral bandwidth. However, reconstruction using filters with different transmittance profiles may yield different reconstruction results because of the performed approximations. Many authors[4,5,13-15] have studied the influence of these filters in the visible region, since they constitute a basic component of many color reproduction systems. In the NIR region, the choice of the filters is only conditioned by the quality of reconstruction of the spectral curves, as no colorimetric space is defined in the studied region, and simple transmittance profiles are used in order to obtain available commercial filters.

In this study, we present a multispectral imaging based method for reconstructing the spectral reflectance curves of samples in the 800-1000 nm range, using measurements performed with a conventional CCD camera. We compare various existing mathematical methods such as the Wiener estimation, non-linear methods and principal component analysis. We analyze the number and shape of the filters to be used in various channels in order to obtain good reconstructions in the NIR region. We use simple transmittance profiles in order to obtain available commercial filters. Using numerical simulation, we analyze the reconstruction results that would be obtained for 30 spectral curves with different sets of filters, under the influence of two different illuminants with color temperatures Tc_1 = 2852K and Tc_2 = 3371K. To date, no spectral reconstruction methods in the NIR region using conventional CCD camera measurements have been reported.

2. METHODOLOGY

2.1 Spectral reconstruction

The reconstruction method is summarized in Figure 1. A multi-channel image of an original object is acquired by placing a selected set of filters in front of the camera. Then, a spectral reconstruction method is applied and the reconstructed spectral reflectance of the sample is obtained.

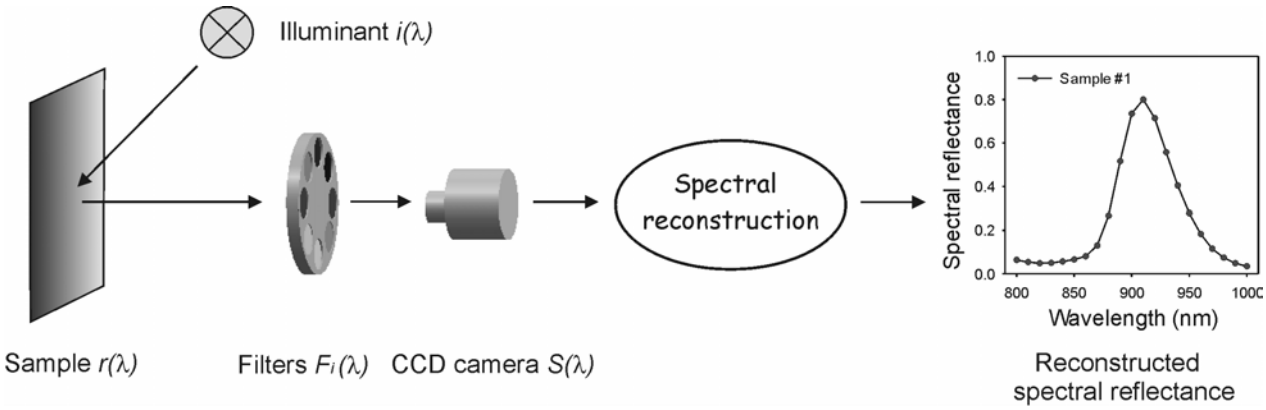

Figure 1: Schematic view of the acquisition system and the final spectral reconstruction step.

Essentially, three reconstruction methods are studied in this work: the Wiener estimation, the non-linear methods and principal component analysis. They are all estimation methods, and therefore they can be applied by using non-monochromatic filters. Consequently, the CCD camera responses for each channel can be expressed as follows:

$$X_i = \int_{\lambda_{min}}^{\lambda_{max}} i(\lambda) r(\lambda) \tau(\lambda) F_i(\lambda) S(\lambda) \, \mathrm{d}\lambda \,, \tag{1}$$

where X_i is the digital level obtained for a certain channel ($i = 1,...,m$), $i(\lambda)$ is the spectral radiance of the illuminant, $r(\lambda)$ is the spectral reflectance of the sample, $\tau(\lambda)$ is the spectral transmittance of the optical path, $F_i(\lambda)$ is the spectral transmittance of the filters placed between the camera and the sample (different for each channel), and $S(\lambda)$ is the spectral sensitivity of the CCD camera used. The term $\tau(\lambda)$ includes the optical system in front of the camera (objective lens) as well as the spectral transmittance of the atmosphere. We considered the value of this term to be 1, which is approximately its value in normal conditions.

The spectral radiance of the illuminant, the spectral transmittance of the filter and the spectral sensitivity of the camera can be brought together in a term called $C_i(\lambda)$:

$$C_i(\lambda) = i(\lambda)F_i(\lambda)S(\lambda)\,, \tag{2}$$

and we can write (1) as follows:

$$X_i = \int_{\lambda_{min}}^{\lambda_{max}} C_i(\lambda)r(\lambda)\,\mathrm{d}\lambda\,, \tag{3}$$

for each of the m existing channels of the camera. In matrix notation:

$$X_i = \mathbf{C_i r}\,, \tag{4}$$

where $\mathbf{C_i}$ is a row vector with components $i(\lambda)F_i(\lambda)S(\lambda)$ and $\mathbf{r}$ is a column vector with components $r(\lambda)$, both analyzed at n wavelengths.

In general, we can write:

$$\mathbf{X} = \mathbf{C r}\,, \tag{5}$$

where $\mathbf{X}$ is a column vector which represents the m camera responses to the sample for the m channels (X_i) and $\mathbf{C}$ is a matrix ($m \times n$) whose rows are the spectral sensitivity of each used channel, that is,

$$\mathbf{C} = \begin{bmatrix} i(\lambda_1)F_1(\lambda_1)S(\lambda_1) & \cdots & i(\lambda_n)F_1(\lambda_n)S(\lambda_n) \\ \vdots & & \vdots \\ i(\lambda_1)F_m(\lambda_1)S(\lambda_1) & \cdots & i(\lambda_n)F_m(\lambda_n)S(\lambda_n) \end{bmatrix}. \tag{6}$$

In order to use the three proposed methods, it is necessary to know a set of spectral reflectance data similar to the curves that we want to reconstruct. The set of p known spectral reflectance curves is represented by a matrix ($n \times p$) called the original data matrix ($\mathbf{O_r}$), whose columns are the p known spectra.

In the case of the Wiener estimation, we assume that a matrix $\mathbf{D}$ exists and that it provides the spectral reflectances from the camera responses, that is,

$$\mathbf{O_r} = \mathbf{D X_{Or}}\,, \tag{7}$$

where $\mathbf{X_{Or}}$ is a matrix ($m \times p$) whose columns are the camera responses for each of the known samples for the different existing channels,

$$\mathbf{X_{Or}} = \begin{bmatrix} X_{1,1} & X_{1,2} & . & . & . & X_{1,p} \\ X_{2,1} & X_{2,2} & & & & \\ . & . & & & & . \\ . & . & & & & . \\ . & . & & & & . \\ X_{m,1} & X_{m,2} & . & . & . & X_{m,p} \end{bmatrix} = \mathbf{CO_r} . \tag{8}$$

Combining equations (7) and (8), we obtain:

$$\mathbf{O_r} = \mathbf{DCO_r} . \tag{9}$$

Inverting equation (9) using the pseudoinverse technique[4], which gives the least-norm solution, we obtain a matrix **D** which minimizes the distance between the known and the estimated spectral reflectances:

$$\mathbf{D} = \mathbf{O_r X_{Or}^T (X_{Or} X_{Or}^T)^{-1}} = \mathbf{O_r O_r}^{\mathbf{T}} \mathbf{C^T (CO_r O_r}^{\mathbf{T}} \mathbf{C^T)^{-1}} . \tag{10}$$

We assume that the reflectance spectra to be reconstructed are a linear combination of the known spectral curves, that is, the curves belonging to the original data matrix are a good representation of all the spectra. This can be stated as follows:

$$\mathbf{r} \cong \mathbf{O_r \alpha} , \tag{11}$$

where $\boldsymbol{\alpha}$ is a column vector whose components are the coefficients of the linear combination. Therefore, matrix **D** is valid for the reconstruction of any curve **r**,

$$\mathbf{r_{rec}} \cong \mathbf{DX} = \mathbf{DCr} \cong \mathbf{DCO_r \alpha} . \tag{12}$$

The difficulty of this method is finding a set of representative spectral reflectances of the curves to be reconstructed. Otherwise, the performed approximations would not be accurate.

In the Wiener estimation we have used a linear transformation to relate the reflectance spectra to the camera responses (Equations 7 and 8). By extension, we can also apply a non-linear transformation (*non-linear methods*). Instead of using matrix $\mathbf{X_{Or}}$ we can consider a matrix $\mathbf{X_{NL}}$ whose columns are a second or higher order polynomial of the camera responses. Therefore, we can calculate another matrix $\mathbf{D_{NL}}$ which relates the polynomial data to the spectral reflectances. Using a complete second order polynomial and three available channels, matrix $\mathbf{X_{NL}}$ would be:

$$\mathbf{X_{NL}} = \begin{bmatrix} 1 & 1 & . & . & . & 1 \\ X_{1,1} & X_{1,2} & . & . & . & X_{1,p} \\ X_{2,1} & X_{2,2} & . & . & . & X_{2,p} \\ X_{3,1} & X_{3,2} & . & . & . & X_{3,p} \\ X_{1,1}^2 & X_{1,2}^2 & . & . & . & X_{1,p}^2 \\ X_{2,1}^2 & X_{2,2}^2 & . & . & . & X_{2,p}^2 \\ X_{3,1}^2 & X_{3,2}^2 & . & . & . & X_{3,p}^2 \\ X_{1,1}X_{2,1} & X_{1,2}X_{2,2} & . & . & . & X_{1,p}X_{2,p} \\ X_{1,1}X_{3,1} & X_{1,2}X_{3,2} & . & . & . & X_{1,p}X_{3,p} \\ X_{2,1}X_{3,1} & X_{2,2}X_{3,2} & . & . & . & X_{2,p}X_{3,p} \end{bmatrix} . \tag{13}$$

We can use polynomials of any order or shape. In practice, this is limited by the required precision and the computational cost. The intersection between channels is often small and therefore, an increase in the order of the

polynomial may not result in a significant improvement of the reconstructions.The calculation of matrix $\mathbf{D_{NL}}$ is performed as in the Wiener estimation:

$$\mathbf{D_{NL}} = \mathbf{O_r}\mathbf{X_{NL}^T}(\mathbf{X_{NL}}\mathbf{X_{NL}^T})^{-1}. \tag{14}$$

Principal component analysis associates the matrix $\mathbf{O_r}$ to a vector space and its characteristic vectors can be calculated. By using the whole set of characteristic vectors, it is possible to recover the original vector space in its totality. It is demonstrated that the characteristic vectors that allow the best reconstruction of the spectra are those corresponding to the variance-covariance matrix of the corrected matrix ($\mathbf{O_{rc}}$), that is, $(1/p)\mathbf{O_{rc}}\mathbf{O_{rc}^t}$. $\mathbf{O_{rc}}$ is the same matrix as $\mathbf{O_r}$, but the mean column vector $\mathbf{r_M}$ (which represents the average of the original p curves) has been extracted from its columns. In order to reconstruct each of the curves belonging to the original data matrix or spectra similar to them ($\mathbf{r}$), each characteristic vector calculated must be added in the proper amounts (using linear combination) to the mean curve or vector $\mathbf{r_M}$. In vector notation this can be stated as follows:

$$\mathbf{r} \cong \mathbf{r_M} + \alpha\mathbf{v_{r1}} + \beta\mathbf{v_{r2}} + \gamma\mathbf{v_{r3}} + \delta\mathbf{v_{r4}} + ... + \xi\mathbf{v_{rq}}, \quad q \le n, \tag{15}$$

where $\alpha, \beta, ..., \xi$ are scalar coefficients and $\mathbf{v_{r1}}$, $\mathbf{v_{r2}}$, ..., $\mathbf{v_{rq}}$ are the characteristic vectors. The scalar coefficients are the amounts of the characteristic vectors which must be combined in order to recover each spectral curve.

In order to explain the differences along all the spectral curves it would be necessary to equate q to n, because of the vector space definition. It is demonstrated that a small set of characteristic vectors can explain a large percentage of variability in the curves, and for this reason, from now on we shall assume that $q < n$. This is normally due to the fact that not all the spectra of the original data matrix are linearly independent.

Combining equations (5) and (15), we obtain a relation between the camera responses and the calculated characteristic vectors:

$$\mathbf{X} = \mathbf{Cr} \approx \mathbf{Cr_M} + \alpha\mathbf{Cv_{r1}} + \beta\mathbf{Cv_{r2}} + \gamma\mathbf{Cv_{r3}} + ... + \xi\mathbf{Cv_{rq}}, \quad q < n, \tag{16}$$

We know all the variables of Equation (16) except the scalar coefficients $\alpha, \beta, ..., \xi$. We have the same number of scalar coefficients as characteristic vectors that we want to use in the reconstruction. In order to find the value of these coefficients, the same number of equations as unknown quantities is needed (the same number of channels or filters as characteristic vectors used in the reconstruction). After these coefficients are calculated, we can apply Expression (15) to reconstruct $\mathbf{r}$, and consequently determine the spectrum of the unknown sample.

In order to evaluate the quality of the reconstruction we use two different parameters :

$$\text{Percentage of reconstruction: } P_{rec} = \left[1 - \frac{\sum_{\lambda_{min}}^{\lambda_{max}}(r - r_{rec})^2}{\sum_{\lambda_{min}}^{\lambda_{max}}(r)^2}\right] \times 100, \tag{17}$$

$$\text{Root Mean Square Error: } RMSE = \left[\frac{1}{N_\lambda}\sum_{\lambda_{min}}^{\lambda_{max}}(r - r_{rec})^2\right]^{1/2}, \tag{18}$$

where r are the experimental components of the original reflectance curves, r_{rec} are the reconstructed values and N_λ are the number of wavelengths where the measurements are made.

RMSE is a commonly used parameter in multispectral imaging and provides a non-limited value related to the difference between the original and the reconstructed spectra. The percentage of reconstruction provides a more intuitive idea of the quality of the reconstruction since its maximum possible value is 100. However, the percentage of reconstruction parameter is very sensitive to variations and in some cases a percentage of 99% or less can lead to considerable differences between the original and the reconstructed spectra.

2.2 Choice of filters

The reconstruction of spectra explained above involves the use of various acquisition channels and therefore different filters. Some authors have studied the influence of the filters in the visible region, in order to use the camera responses as colorimetric values[4,5,13-15]. In the NIR region, the choice of the filters is only conditioned by the quality of reconstruction of the spectral curves, as no colorimetric space is defined in this range, and we use simple transmittance profiles in order to obtain available commercial filters. For this purpose, we can choose equi-spaced Gaussian filters. In order to simplify the choice we will define some conditions beforehand. We consider that the filters used have the following transmittance:

$$T(\lambda) = T_{MAX} \exp\left[-0.5\left(\frac{\lambda - \lambda_0}{\Delta\lambda} \right)^2 \right], \tag{19}$$

where T_{MAX} is the maximum height of the Gaussian peak, λ_0 is the wavelength corresponding to the maximum (center) of the Gaussian and $\Delta\lambda$ is related to the full width-half maximum (FWHM) of the Gaussian.

The ideal supposed maximum transmittance (T_{MAX}) is 1. In this case, each channel has a different sensitivity. The filters are considered equispaced in the 800-1000 nm region, and parameter λ_0 is therefore also fixed according to the number of filters used. The parameter $\Delta\lambda$ is considered as the optimization parameter. It is increased progressively in the same way for all the filters and we choose the value that provides the best reconstruction for the spectral curves belonging to the original data matrix. We can modify parameter $\Delta\lambda$ independently for each filter, but this leads to a high computational cost not justified by the results obtained.

3. DATA

In order to test these spectral reconstruction methods and to estimate the results that they would yield, we performed a simulation of the reconstructions for various textile samples. We analyzed the number and shape of the filters required in order to obtain good spectral reconstructions and optimized the process by searching for the optimum Gaussian filters.

The original data matrix considered for the simulation consisted of 30 spectral curves (Figure 2). Nineteen were real and eleven were theoretical or unreal curves. Compared to visible spectral reflectances, the NIR spectra of samples are normally smooth and repetitive because of its dependency on the chemical composition. However, theoretical curves were chosen in order to obtain larger differences among the original curves and therefore to verify the viability of the method in worse-than-normal conditions. We considered the spectral data between 800 nm and 1000 nm in 10 nm steps. Therefore, each curve was made up of 21 components.

In the simulations, we considered the spectral sensitivity of a progressive scan camera JAI CV-M10 experimentally determined (Figure 3 (a)). The simulated reconstructions were performed using a minimum of 2 and a maximum of 6 filters under the influence of two different halogen lamps with color temperatures $Tc_1 = 2852$ K and $Tc_2 = 3371$ K. These two temperatures cover a wide real range and the results obtained can thus be applied under several lighting conditions. The spectral radiance of both illuminants is represented in Figure 3 (b).

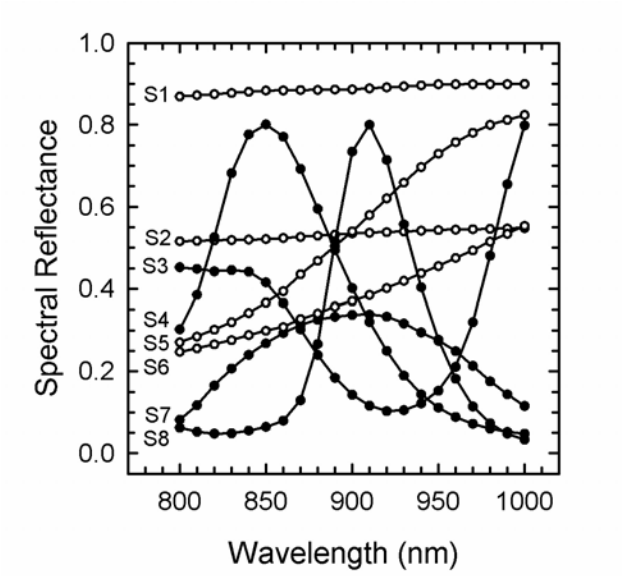

Figure 2: Spectral reflectance curves of 8 representative samples belonging to the original data matrix (white dots correspond to real curves and black dots to theoretical curves).

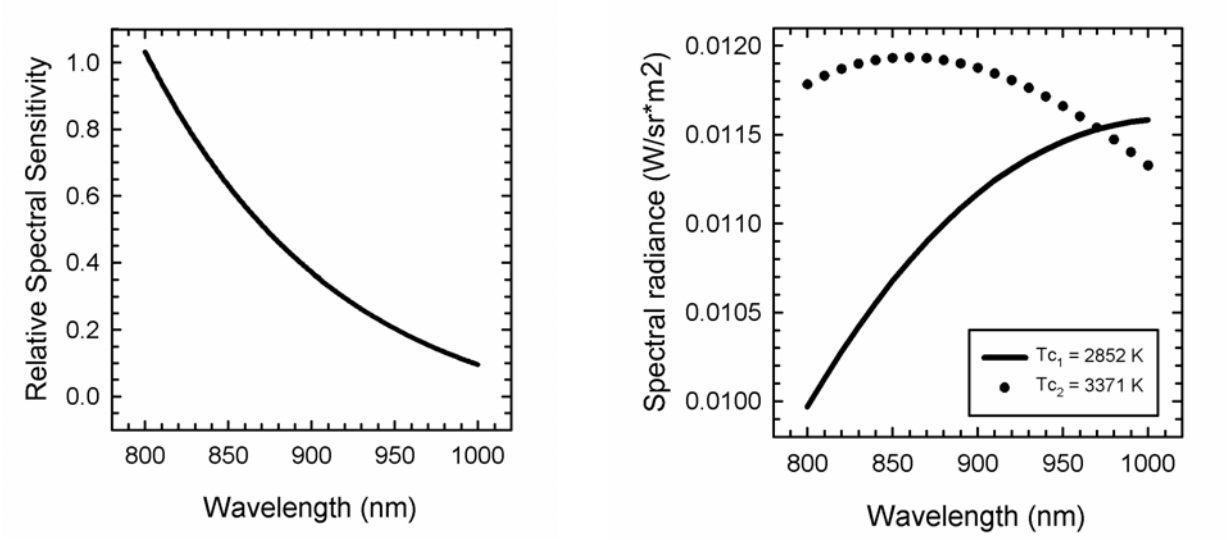

(a) (b)

Figure 3: Experimental relative spectral sensitivity of the camera JAI CV-M10 (a) and spectral radiance of the halogen lamps used in the simulation (b).

The optimization process consisted in searching for the best reconstruction parameters (P_{rec} and *RMSE*) for all the curves belonging to the original data matrix.

4. RESULTS

The simulated results (mean percentage of reconstruction and *RMSE*) obtained for the different existing reconstruction methods using the five optimum filters and the illuminant $Tc_1 = 2852K$ are illustrated in Figure 4. The methods tested were linear interpolation, cubic interpolation, spline interpolation, discrete Fourier transform, and modified discrete sine transform approximations, Moore-Penrose pseudoinverse, smoothing inverse, Wiener estimation, a non-linear method (using a complete second order polynomial) and principal component analysis. It can be seen that the methods with the best reconstruction parameters are the Wiener estimation, the non-linear method and principal component analysis. The numerical results of these three last methods can be seen in Table 1. In this table, the optimum parameter $\Delta\lambda$, the mean, the standard deviation, and the maximum and minimum P_{rec} and *RMSE* values for all the simulated cases are shown. The results are presented under the influence of the two halogen lamps $Tc_1 = 2852$ K and $Tc_2 = 3371$ K and using from 2 to 6 filters. As expected, the reconstructions improve with the use of more filters. It can be seen that the shape of the best filters (parameter $\Delta\lambda$) depends on the number of filters and the reconstruction method used in the simulation process. While Wiener estimation and principal component analysis have similar reconstruction parameters in all the analyzed cases, the non-linear method provides smaller errors.

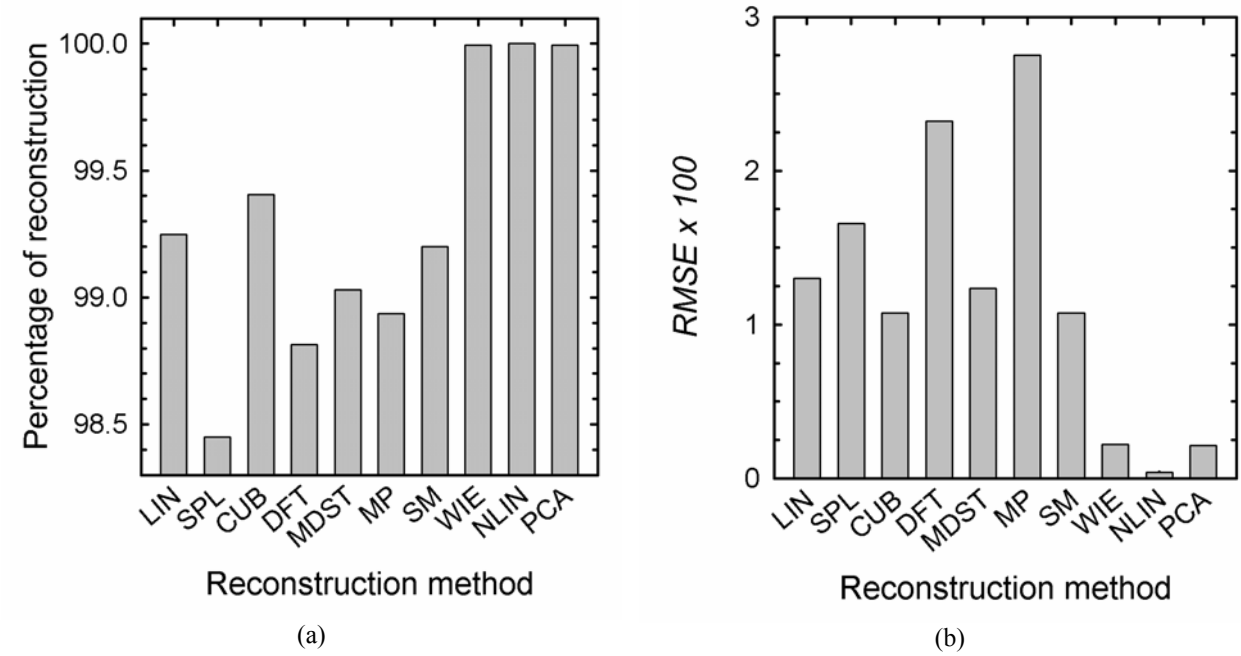

Figure 4: Mean percentage of reconstruction and *RMSE* of the samples which belong to the original data matrix obtained for several existing reconstruction methods (LIN: linear interpolation, SPL: Spline interpolation, CUB: cubic interpolation, DFT: discrete Fourier transform approximation, MDST: modified discrete sine transform approximation, MP: Moore-Penrose pseudoinverse, SM: smoothing inverse, WIE: Wiener estimation, NLIN: non-linear method (using a complete second order polynomial) and PCA: principal component analysis) using the illuminant of color temperature $Tc_1 = 2852$ K, and the five optimum filters

The evolution of the parameter *RMSE* according to the number of filters used is represented in Figure 5. With two filters, all three methods have high *RMSE* values and a large standard deviation. In the case of Wiener estimation and principal component analysis, the results improve using three and four filters, although they still present high dispersion. With five filters, $RMSE \times 100$ is smaller than 1 and has little deviation in all the analyzed cases. Even though the reconstructions improve further with the use of six filters, the changes are very small and *RMSE* is almost constant. The use of three filters with the non-linear method guarantees that $RMSE \times 100$ value is similar to 1 for all the cases analyzed. It can be shown that a $RMSE \times 100$ similar to 1 leads to an almost perfect reconstruction of the spectral reflectance of the samples. A $RMSE \times 100$ similar to 1 is equivalent to a percentage of reconstruction of about 99.9%.

WIENER	LAMP Tc_1 = 2852 K					LAMP Tc_2 = 3371 K				
Number of filters	**2**	**3**	**4**	**5**	**6**	**2**	**3**	**4**	**5**	**6**
$\Delta\lambda$	100	28	100	28	65	100	27	100	26	62
Mean P_{rec}	93.426	98.969	99.649	99.994	99.997	93.363	98.955	99.652	99.993	99.997
Std Dev P_{rec}	10.631	1.700	0.974	0.013	6.539	10.391	1.754	0.970	0.013	6.447e-3
Max P_{rec}	99.988	99.981	99.998	100	100	99.988	99.981	99.998	100	100
Min P_{rec}	65.949	90.999	94.976	99.934	99.966	66.977	90.680	94.974	99.937	99.967
Mean (*RMSE100)**	6.468	3.178	1.179	0.221	0.122	6.566	3.191	1.183	0.229	0.123
Std Dev (*RMSE100)**	5.378	2.159	1.658	0.206	0.123	5.401	2.186	1.648	0.211	0.123
Max (*RMSE100)**	20.833	11.39	8.510	0.815	0.474	20.516	11.591	8.512	0.877	0.470
Min (*RMSE100)**	0.957	1.187	0.243	0.043	0.014	0.951	1.201	0.250	0.043	0.015
NON-LINEAR	LAMP Tc_1 = 2852 K					LAMP Tc_2 = 3371 K				
Number of filters	**2**	**3**	**4**	**5**	**6**	**2**	**3**	**4**	**5**	**6**
$\Delta\lambda$	5	13	54	28	29	5	13	57	27	33
Mean P_{rec}	96.616	99.943	99.998	100	100	96.617	99.943	99.998	100	100
Std Dev P_{rec}	5.605	0.180	5.107e-3	2.705e-4	8.016e-5	5.603	0.179	4.547e-3	2.935e-4	8.200e-5
Max P_{rec}	99.998	100	100	100	100	99.998	100	100	100	100
Min P_{rec}	79.966	99.011	99.978	99.999	100	79.965	99.016	99.982	99.999	100
Mean (*RMSE100)**	4.802	0.600	0.116	0.041	0.025	4.802	0.600	0.115	0.043	0.024
Std Dev (*RMSE100)**	3.712	0.381	0.079	0.026	0.020	3.712	0.381	0.078	0.028	0.019
Max (*RMSE100)**	13.548	1.504	0.325	0.089	0.079	13.545	1.503	0.329	0.093	0.072
Min (*RMSE100)**	0.374	0.081	0.018	2.309e-3	1.574e-3	0.374	0.081	0.019	2.422e-3	1.234e-3
PCA	LAMP Tc_1 = 2852 K					LAMP Tc_2 = 3371 K				
Number of filters	**2**	**3**	**4**	**5**	**6**	**2**	**3**	**4**	**5**	**6**
$\Delta\lambda$	100	29	65	28	24	100	28	68	26	24
Mean P_{rec}	93.105	99.110	99.719	99.995	99.997	92.802	99.098	99.722	99.994	99.997
Std Dev P_{rec}	13.502	1.393	0.719	0.010	4.633e-3	14.162	1.418	0.710	0.010	4.694e-3
Max P_{rec}	99.973	99.991	100	100	100	99.973	99.991	100	100	100
Min P_{rec}	53.922	94.632	96.180	99.948	99.983	51.322	94.508	96.229	99.950	99.983
Mean (*RMSE100)**	5.936	2.725	1.305	0.215	0.173	6.080	2.737	1.298	0.223	0.174
Std Dev (*RMSE100)**	5.630	1.776	0.951	0.207	0.177	5.745	1.787	0.945	0.212	0.179
Max (*RMSE100)**	25.772	8.285	4.220	0.773	0.706	26.489	8.370	4.196	0.834	0.711
Min (*RMSE100)**	1.293	0.822	0.133	0.044	0.024	1.295	0.833	0.133	0.047	0.024

Table 1: Parameter $\Delta\lambda$ of the filters with the best reconstruction, mean, standard deviation, maximum and minimum P_{rec}, and *RMSE* values for the studied methods (WIENER: Wiener estimation, NON-LINEAR: non-linear method (using a complete second order polynomial), PCA: principal component analysis). Number of filters used: between two and six, and illuminants with Tc_1 = 2852 K and Tc_2 = 3371 K.

Figure 6 shows the spectral sensitivity for each of the three optimum channels using the non-linear method, and for the five optimum channels in the case of principal component analysis. The spectral sensitivity was calculated taking into account the spectral response of the camera JAI CV-M10, the emitted spectral radiance of the illuminant Tc_1 = 2852K and the transmittance of the corresponding optimum filters obtained. The optimum filters obtained have a large spectral width and are therefore easily commercially available.

Examples of reconstructed spectral reflectances with two and three filters using the non-linear method and two and five filters using principal component analysis are illustrated in Figure 7. While there are large differences between the original and the reconstructed spectra using two filters, the reconstructed spectra with three and five filters and the original spectra are almost the same.

We noticed that the results were fairly independent of the illuminant used. This low dependency may be due to the smoother spectral distribution of the radiance of the illuminant compared to the spectral reflectance of the samples. The reconstruction parameters have similar values in both cases, and the best filters are almost the same (the same value for parameter $\Delta\lambda$). This indicates that with the same set of filters we can obtain good reconstructions for every type of illuminant.

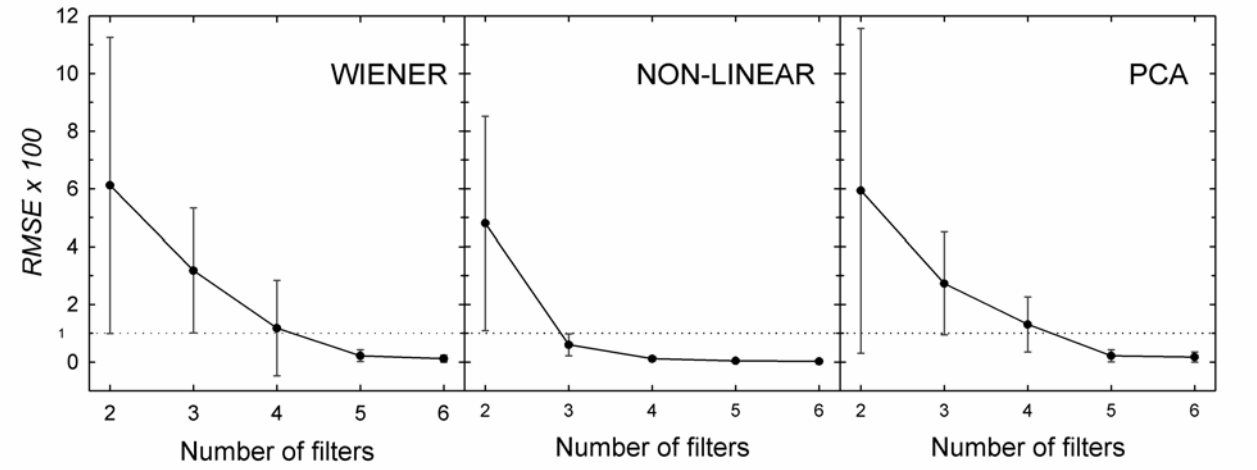

Figure 5: Evolution of mean *RMSE × 100* and the corresponding standard deviation according to number of filters, using Wiener estimation, the non-linear method and principal component analysis. The illuminant used is $Tc_1 = 2852$ K.

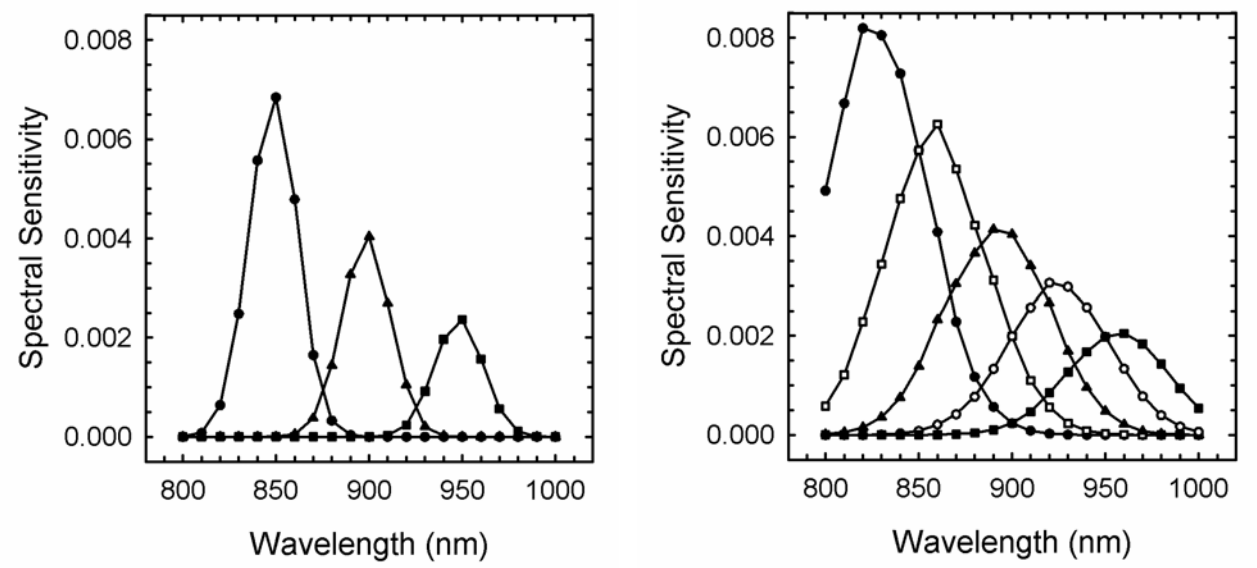

(a) (b)

Figure 6: Spectral sensitivity of the three optimum channels ($\Delta\lambda = 13$ or FWHM ≈ 31 nm) using the non-linear method (a) and the five optimum channels ($\Delta\lambda = 28$ or FWHM ≈ 66 nm) using principal component analysis (b). The sensitivity includes the spectral response of the JAI CV-M10 camera, the emitted spectral radiance of the illuminant ($Tc_1 = 2852$ K) and the transmittance of the optimum filters.

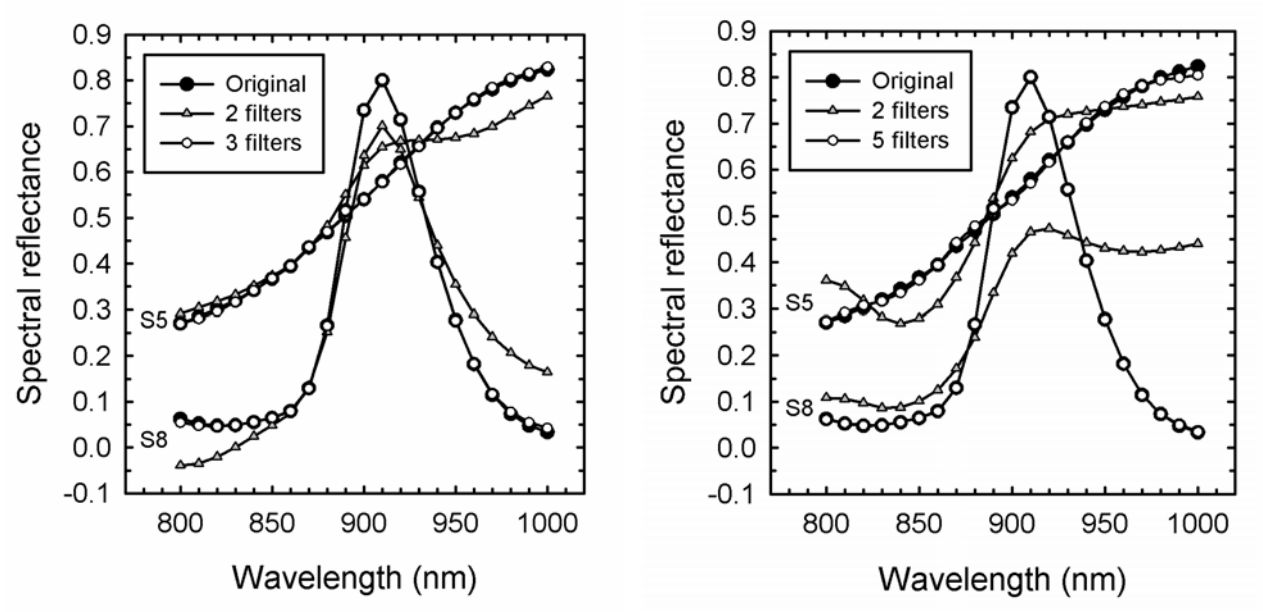

(a) (b)

Figure 7: Reconstructions of samples S5 and S8 of the original data matrix with 2 and 3 filters using the non-linear method (a) and 2 and 5 filters using principal component analysis (b). The illuminant used is $Tc_1 = 2852$ K.

5. CONCLUSIONS

We have presented a method for reconstructing the spectral reflectance of samples in the NIR region of the spectrum. We used a method based on multispectral imaging which involves the use of three or more acquisition channels of a conventional CCD camera. We have analyzed different mathematical methods for reconstructing the spectral data. The methods which yield the best reconstruction results are Wiener estimation, non-linear methods and principal component analysis. We performed an optimization process using numerical simulation in order to determine the number and shape of filters which give the best reconstruction parameters (P_{rec} and *RMSE*). We analyzed the reconstructions of 30 samples using from 2 to 6 equi-spaced Gaussian filters under the influence of two different illuminants with color temperatures $Tc_1 = 2852$K and $Tc_2 = 3371$K. The bandwidth of the Gaussian filters was optimized in order to obtain the best reconstruction parameters. As expected, the reconstruction of the curves improves if the number of acquisition channels is increased. Using three filters in the case of the non-linear method (second order polynomial) and five filters in the case of Wiener estimation and principal component analysis, the reconstructed reflectance spectra are very similar to the original curves. In these cases, the mean $RMSE \times 100$ is smaller than 1 and the mean percentage of reconstruction is higher than 99.9%. The shape of the optimum filters depends on the number of channels used, but in all the studied cases they have a large spectral bandwidth. Moreover, parameter $\Delta\lambda$ is almost independent of the illuminant used. This makes the method widely applicable, since the reconstructions may be performed under many lighting conditions using the same set of filters. Therefore, we have demonstrated that using a conventional CCD camera and filters with a large spectral bandwidth, and therefore commercially available, it is possible to obtain good spectral reflectance reconstructions in the NIR region. The number of optimum filters necessary to obtain good reconstructions depends on the method used (at least three using the non-linear method and five for the other methods).

ACKNOWLEDGMENTS

This research was supported by the Comisión Interministerial de Ciencia y Tecnología (CICYT) (Spain) under grant TAP-99-0856.

REFERENCES

1. G. C. Holst, *CCD Arrays, cameras and displays*, SPIE Press, Bellingham, WA, 1998.
2. J. M. Pope, "NIR gains continue in on-line process applications", *Chiltons I&CS*, **67**(2), 45-47, 1994.
3. M. Matsuoka, *Infrared absorbing dyes*, Plenum Press, New York, 1990.
4. J. Y. Hardeberg, *Acquisition and reproduction of color images: colorimetric and multispectral approaches*, Ph.D dissertation , École Nationale Supérieure des Télécommunications, Paris, 1999.
5. M. J. Vrhel and H. J. Trussell, "Filter considerations in color correction*", IEEE Transactions on Image Processing* **3**(2), 147-161, 1994.
6. F. König and W. Praefcke, "The practice of multispectral image acquisition", in *EUROPTO Conference on Electronic Imaging: Processing, Printing and Publishing in Color* (Zürich, Switzerland), Proc. SPIE **3409**, 34-41, 1998.
7. G. Hong, M. R. Luo and P. A. Rhodes, "A study of digital camera colorimetric characterization based on polynomial modeling", *Color Research and application* **26**(1), 76-84, 2001.
8. P. G. Herzog, D. Knipp, H. Stiebig and F. König, "Colorimetric characterization of novel multiple-channel sensors for imaging and metrology", *Journal of Electronic Imaging* **8**(4), 342-353, 1999.
9. J. L. Simonds, "Application of characteristic vector analysis to photographic and optical response data", *Journal of the Optical Society of America* **53**(8), 968-974, 1963.
10. M. Vilaseca, J. Pujol and M. Arjona, "Spectral reflectance reconstruction in the NIR region using conventional CCD camera measurements", submitted to *Applied Optics*, April 2002.
11. J. P. S. Parkkinen, J. Hallikainen and T. Jaaskelainen, "Characteristic spectra of Munsell colors", *Journal of the Optical Society of America A* **6**(2), 318-322, 1989.
12. C. Chiao, D. Osorio, M. Vorobyev and T. W. Cronin, "Characterization of natural illuminants in forests and the use of digital video data to reconstruct illuminant spectra", *Journal of the Optical Society of America A* **17**(10), 1713-1721, 2000.
13. M. Wolski, C. A. Bouman, J. P. Allebach and E. Walowit, "Optimizations of sensor response functions for colorimetry of reflective and emissive objects", *IEEE Transactions on Image Processing* **5**(3), 507-517, 1996.
14. P. L. Vora and H. J. Trussell, "Mathematical methods for the design of color scanning filters", *IEEE Transactions on Image Processing* **6**(2), 312-320, 1997.
15. P. L. Vora and H. J. Trussell, "Mathematical methods for the analysis of color scanning filters", *IEEE Transactions on Image Processing* **6**(2), 321-327, 1997.